

## **SUPPORTING INFORMATION**

### **CYCLOSTREPTIN DERIVATIVES SPECIFICALLY TARGET CELLULAR TUBULIN AND FURTHER MAP THE PACLITAXEL SITE**

Enrique Calvo, Isabel Barasoain, Ruth Matesanz, Benet Pera, Emilio Camafeita, Oriol Pineda, Ernest Hamel, Christopher D. Vanderwal, José Manuel Andreu, Juan A. López, José Fernando Díaz

## Supplementary Experimental Procedures

**PIS of peptides cross linked to Cs derivatives.** For the precursor ion scanning (PIS) experiments as shown in Figure 4, the first quadrupole (Q1) of the Applied 4000 Q-Trap triple quadrupole was selected to analyse all peptides under a wide mass range, from 390 to 1200  $m/z$ , while the corresponding diagnostic ion for each Cs derivative compound was selected in the third quadrupole (Q3). Thus, for the ion filtering of peptides bound to Cs derivatives, Q3 was selected to detect the fragment ions at 249  $m/z$  as determined (Figure S3). The parameters for the analyses were set as follows: declustering potential 90 V, entrance potential 10 V, collision energy 35 V, collision cell exit potential 5 V.

**SRM of Cs derivative-bound peptides.** For the targeted detection and quantification of specific, low abundance peptides in highly complex peptides mixtures, SRM is the best choice because of increased sensitivity and selectivity. A specific ion of interest (precursor ion) is selected in the first quadrupole (Q1), followed by a specific fragment ion derived from the precursor (fragment ion) for filtering in the third quadrupole (Q3) after CID. These transitions (precursor/fragment ion pairs) are monitored, and leads to significantly enhanced detection sensitivity and quantitative. Furthermore, to avoid the potential detector saturation of the mass spectrometer and increase the quantitative sensitivity of the SRM analyses, digested samples were diluted 1:10 with buffer A (A= 0.5%  $\text{CH}_3\text{COOH}$  in water). For SRM targeted analyses, Q1 was set on the masses corresponding to tubulin-derived tryptic peptides bound to Cs derivatives previously determined in the PIS experiments. Q3 was set on the marker filtering ion at 249  $m/z$ .

**Modelling of the transition state of the covalent reaction.** The transition state of the attack of methanethiol on methyl chloroacetate was calculated in implicit ethanol using

Spartan '08, version 1.1.2, build 131 (1-2). The calculation was performed with the B3LYP (3-6) functional using the 6-31G\* (7-16) basis set and the SM8 model for solvation (17). Transition state was confirmed by the presence of one imaginary frequency mode. The S–C–Cl angle was 175.27° and approach of methane thiol displaced the chloride, and vice versa. The carbon–sulfur bond length was found to be 2.393 Å

### Supplementary Figures

**Figure S1. Analysis of the tubulin-linked Cs derivative adducts by MALDI-TOF MS.** MALDI spectra show the corresponding Cs-interacting tryptic peptide for each derivative (boxed labels).

**Figure S2. Characterization of Cs derivatives by MS.** Enhanced resolution scan of the 8Ac-Cs (Panel A) and the two chloroacetylated (Panel B) Cs derivatives. Panels C and D show the corresponding enhanced product ion MS/MS spectra. Possible diagnostic ions for further precursor ion filtering experiments are marked (masses at 249 and 365  $m/z$ ).

**Figure S3. Optimization of the PIS experiments.** Detection of the Cs derivatives by PIS experiments is shown. A) Filtering of the 8Ac-Cs using two different fragment diagnostic ions at 249  $m/z$  and 365  $m/z$ . B) Detection of 6CA- and 8CA-Cs by PIS using the diagnostic ions at 249, 365 and 234  $m/z$ . Experiments were performed optimizing acquisition parameters to detect the parental Cs derivative with minimal background. Parental Cs derivatives are marked with an asterisk (\*).

**Figure S4. Analysis of the high resolution adduct signals.** High resolution peaks corresponding to triply-charged tubulin-derived tryptic peptides linked to Cs derivatives

analyzed with a hybrid orbital ion trap. Masses were measured with an error tolerance of 10 ppm.

**Figure S5. Fragmentation spectra of ion 2\*.** Main fragmentation series (y-carboxy and b-amino) are indicated. Water loss ions are labeled with an asterisk and some fragments from Cs derivative dissociation are marked (numbered boxed).

**Figure S6. MS-analysis of microtubules incubated with 6CA-Cs and 8CA-Cs after blocking of the binding site with Cs.** Extracted ion chromatograms for the signals at  $m/z$  1017.855 and 1031.186 corresponding to tubulin adducts bound to Cs and its chloroacetylated derivatives, respectively.

**Figure S7. MS analyses of Cs derivatives bound to oligomeric tubulin by SRM.** Extracted ion chromatogram for MRM experiments of 3 ion pairs, including the ion pair corresponding to tubulin-derived unmodified tryptic peptide (Q1 884  $m/z$ , Q3 836  $m/z$ , labeled as Ctrl) in oligomeric tubulin samples. Numbers above chromatographic peaks indicate the retention time (in brackets) and the type of detected ion.

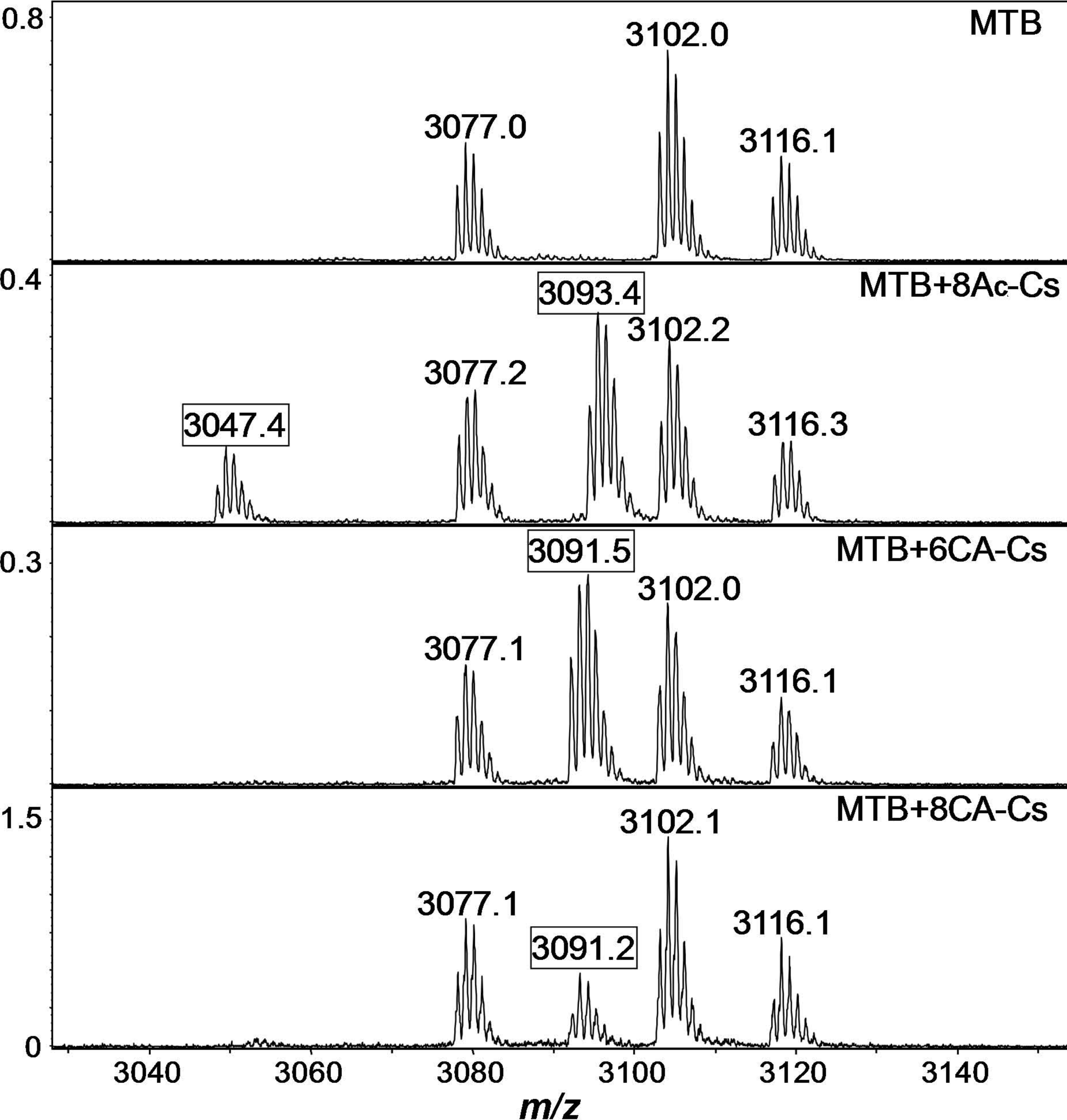
### Supplementary References

1. (2008) Spartan '08, Wavefunction, Inc. Irvine, CA.
2. Shao, Y., Molnar, L. F., Jung, Y., Kussmann, J., Ochsenfeld, C., Brown, S. T., Gilbert, A. T. B., Slipchenko, L. V., Levchenko, S. V., O'Neill, D. P., DiStasio, R. A., Lochan, R. C., Wang, T., Beran, G. J. O., Besley, N. A., Herbert, J. M., Lin, C. Y., Van Voorhis, T., Chien, S. H., Sodt, A., Steele, R. P., Rassolov, V. A., Maslen, P. E., Korambath, P. P., Adamson, R. D., Austin, B., Baker, J., Byrd, E. F. C., Dachsel, H., Doerksen, R. J., Dreuw, A., Dunietz, B. D., Dutoi, A. D., Furlani, T. R., Gwaltney, S. R., Heyden, A., Hirata, S., Hsu, C. P.,

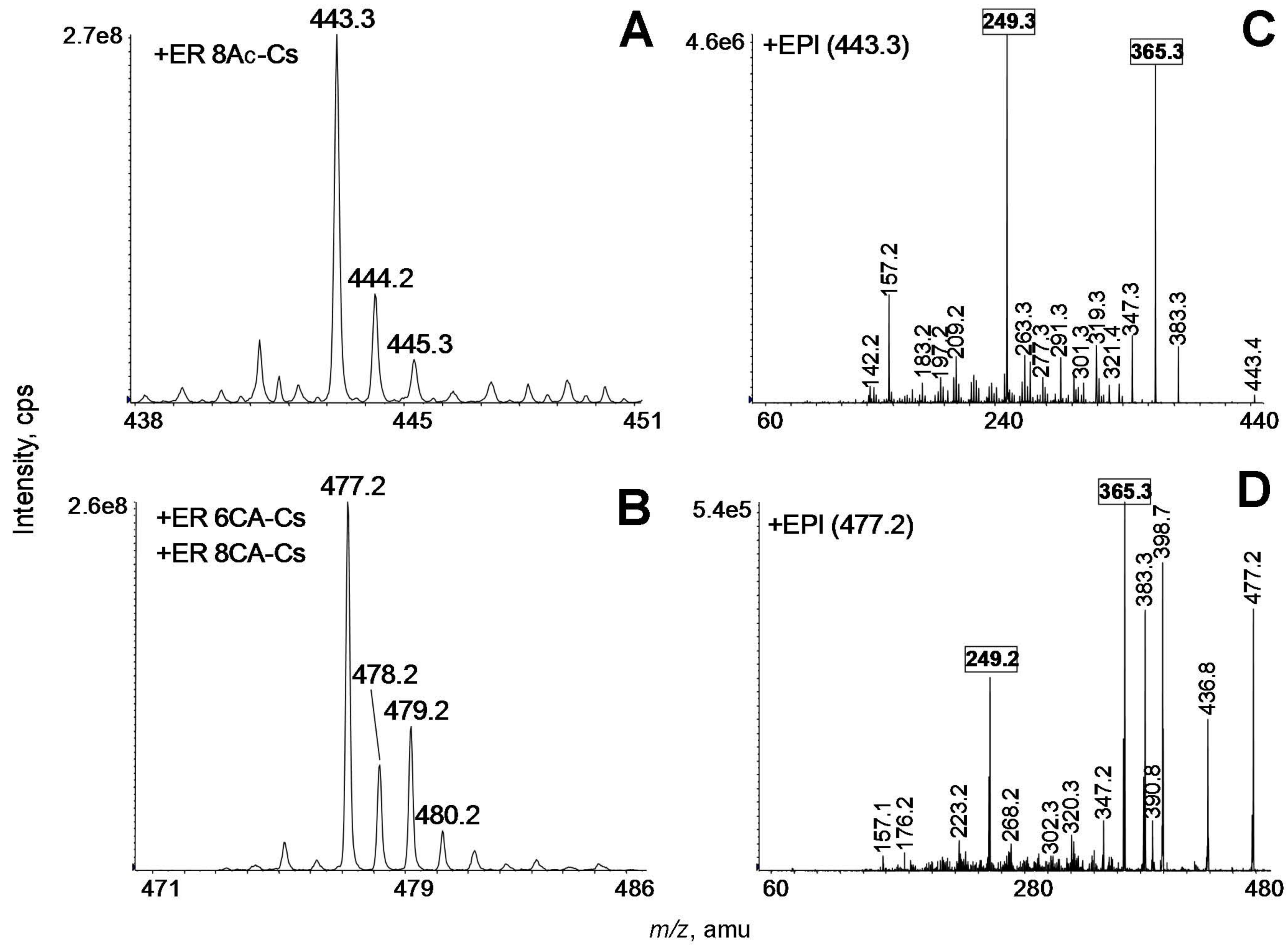
- Kedziora, G., Khalliulin, R. Z., Klunzinger, P., Lee, A. M., Lee, M. S., Liang, W., Lotan, I., Nair, N., Peters, B., Proynov, E. I., Pieniazek, P. A., Rhee, Y. M., Ritchie, J., Rosta, E., Sherrill, C. D., Simmonett, A. C., Subotnik, J. E., Woodcock, H. L., Zhang, W., Bell, A. T., Chakraborty, A. K., Chipman, D. M., Keil, F. J., Warshel, A., Hehre, W. J., Schaefer, H. F., Kong, J., Krylov, A. I., Gill, P. M. W., and Head-Gordon, M. (2006) Advances in methods and algorithms in a modern quantum chemistry program package, *Phys. Chem. Chem. Phys.* 8, 3172-3191.
3. Becke, A. D. (1993) A new mixing of Hartree-Fock and local density-functional theories, *J. Chem. Phys.* 98, 1372-1377.
  4. Lee, C. T., Yang, W. T., and Parr, R. G. (1988) Development of the Colle-Salvetti correlation-energy formula into a functional of the electron-density, *Phys. Rev. B* 37, 785-789.
  5. Vosko, S. H., Wilk, L., and Nusair, M. (1980) Accurate spin-dependent electron liquid correlation energies for local spin-density calculations - a critical analysis, *Can. J. Phys.* 58, 1200-1211.
  6. Stephens, P. J., Devlin, F. J., Chabalowski, C. F., and Frisch, M. J. (1994) Ab-initio calculation of vibrational absorption and circular-dichroism spectra using density-functional force-fields, *J. Phys. Chem.* 98, 11623-11627.
  7. Ditchfield, R., Hehre, W. J., and Pople, J. A. (1971) Self-consistent molecular-orbital methods .9. Extended gaussian-type basis for molecular-orbital studies of organic molecules, *J. Chem. Phys.* 54, 724-&.
  8. Hehre, W. J., Ditchfie.R, and Pople, J. A. (1972) Self-consistent molecular-orbital methods .12. Further extensions of Gaussian-type basis sets for use in molecular-orbital studies of organic-molecules, *J. Chem. Phys.* 56, 2257-&.

9. Harihara, P. C., and Pople, J. A. (1973) Influence of polarization functions on molecular-orbital hydrogenation energies, *Theor. Chim. Acta* 28, 213-222.
10. Harihara, P. C., and Pople, J. A. (1974) Accuracy of AH equilibrium geometries by single determinant molecular-orbital theory, *Mol. Phys.* 27, 209-214.
11. Gordon, M. S. (1980) The isomers of silacyclopropane, *Chemical Physics Letters* 76, 163-168.
12. Francl, M. M., Pietro, W. J., Hehre, W. J., Binkley, J. S., Gordon, M. S., Defrees, D. J., and Pople, J. A. (1982) Self-consistent molecular-orbital methods .23. A polarization-type basis set for 2nd-row elements, *J. Chem. Phys.* 77, 3654-3665.
13. Binning, R. C., and Curtiss, L. A. (1990) Compact contracted basis-sets for 3rd-row atoms - GA-KR, *Journal of Computational Chemistry* 11, 1206-1216.
14. Blaudeau, J. P., McGrath, M. P., Curtiss, L. A., and Radom, L. (1997) Extension of Gaussian-2 (G2) theory to molecules containing third-row atoms K and Ca, *J. Chem. Phys.* 107, 5016-5021.
15. Rassolov, V. A., Pople, J. A., Ratner, M. A., and Windus, T. L. (1998) 6-31G\* basis set for atoms K through Zn, *J. Chem. Phys.* 109, 1223-1229.
16. Rassolov, V. A., Ratner, M. A., Pople, J. A., Redfern, P. C., and Curtiss, L. A. (2001) 6-31G\*basis set for third-row atoms, *Journal of Computational Chemistry* 22, 976-984.
17. Marenich, A. V., Olson, R. M., Kelly, C. P., Cramer, C. J., and Truhlar, D. G. (2007) Self-consistent reaction field model for aqueous and nonaqueous solutions based on accurate polarized partial charges, *Journal of Chemical Theory and Computation* 3, 2011-2033.

Intens. x 10<sup>4</sup>

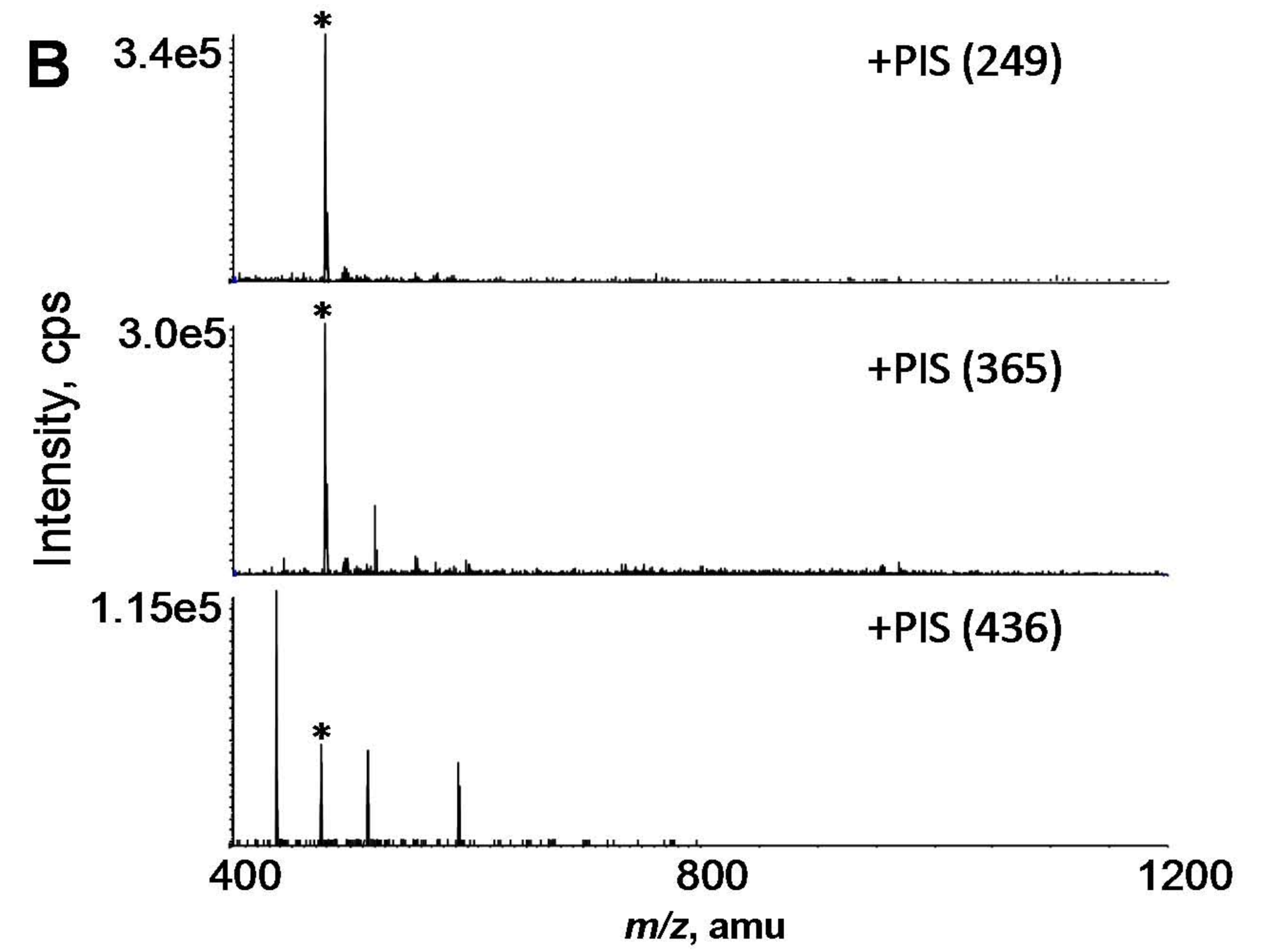
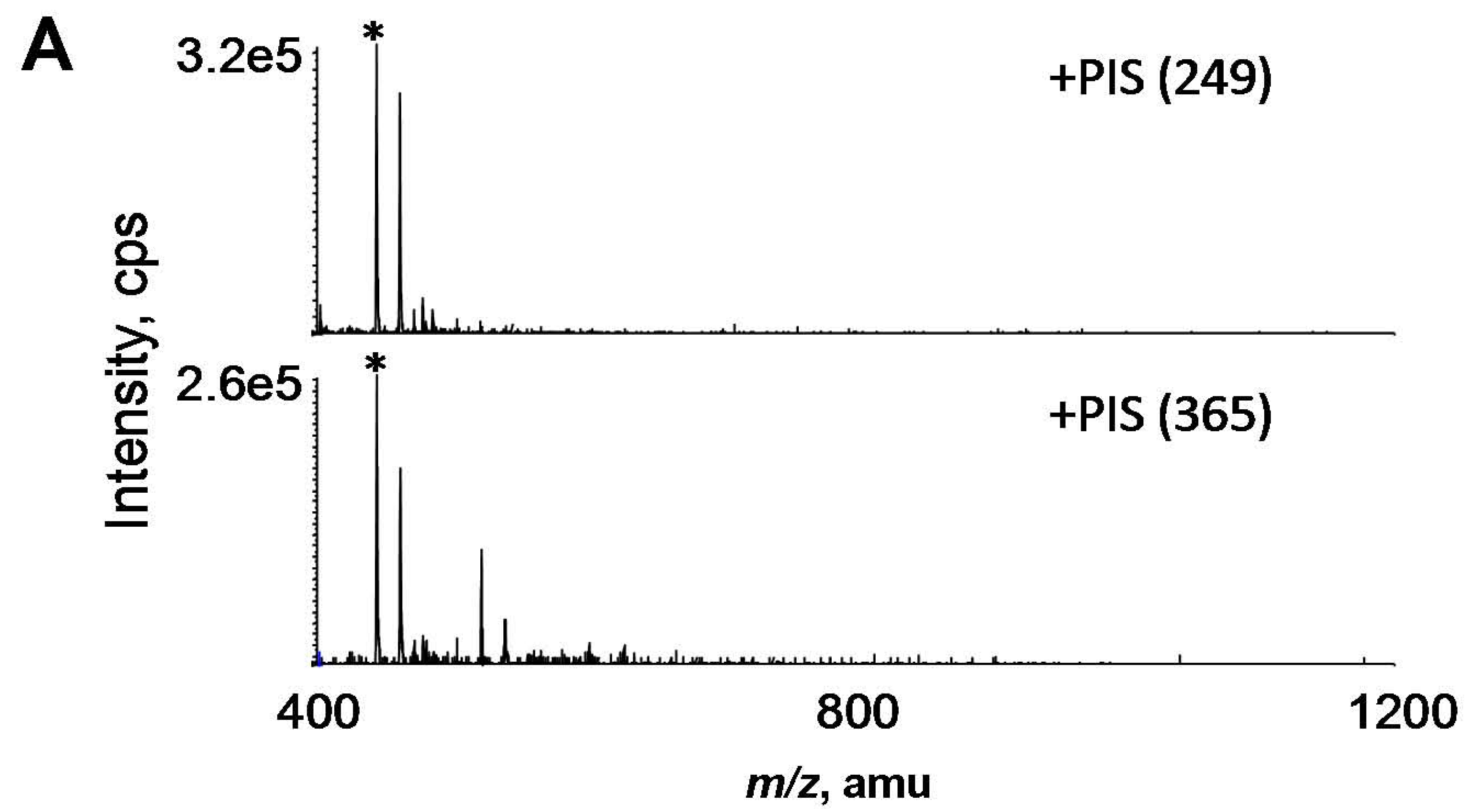


# Supplemental Figure 2

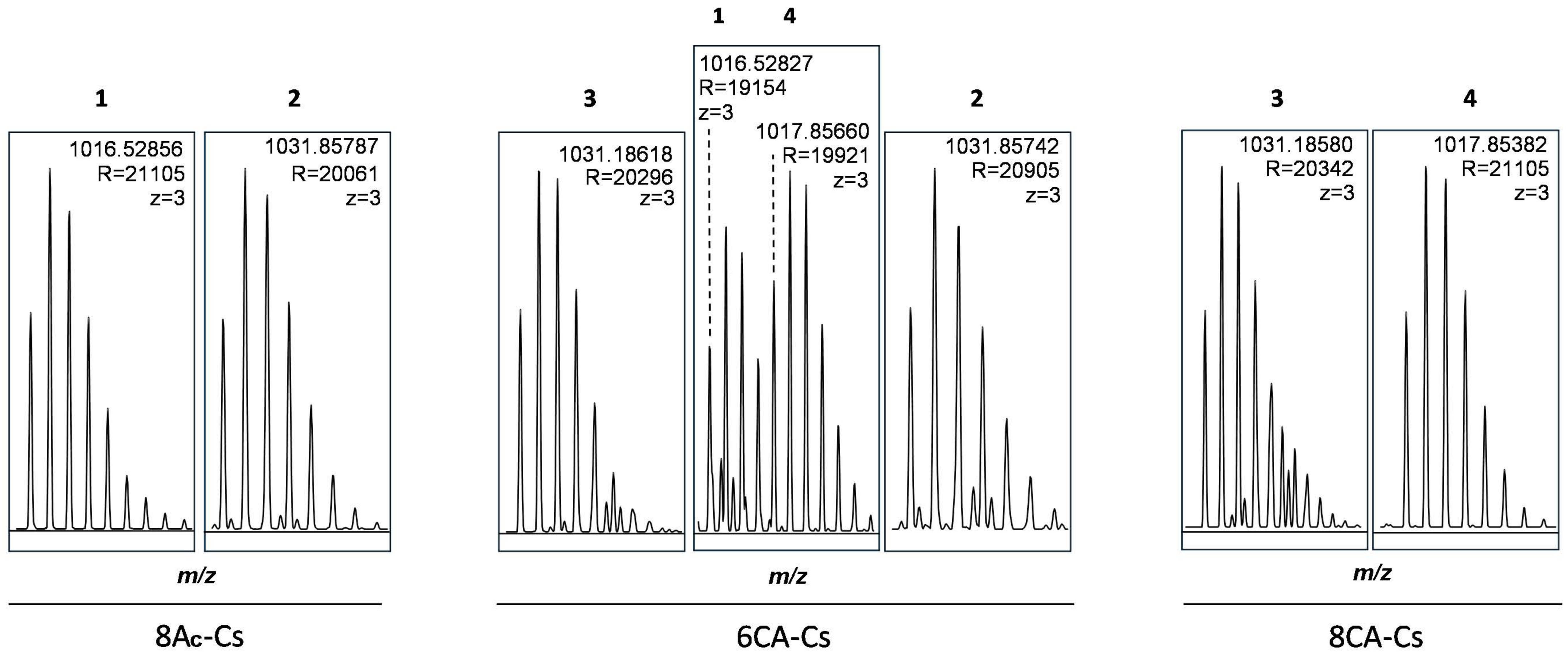


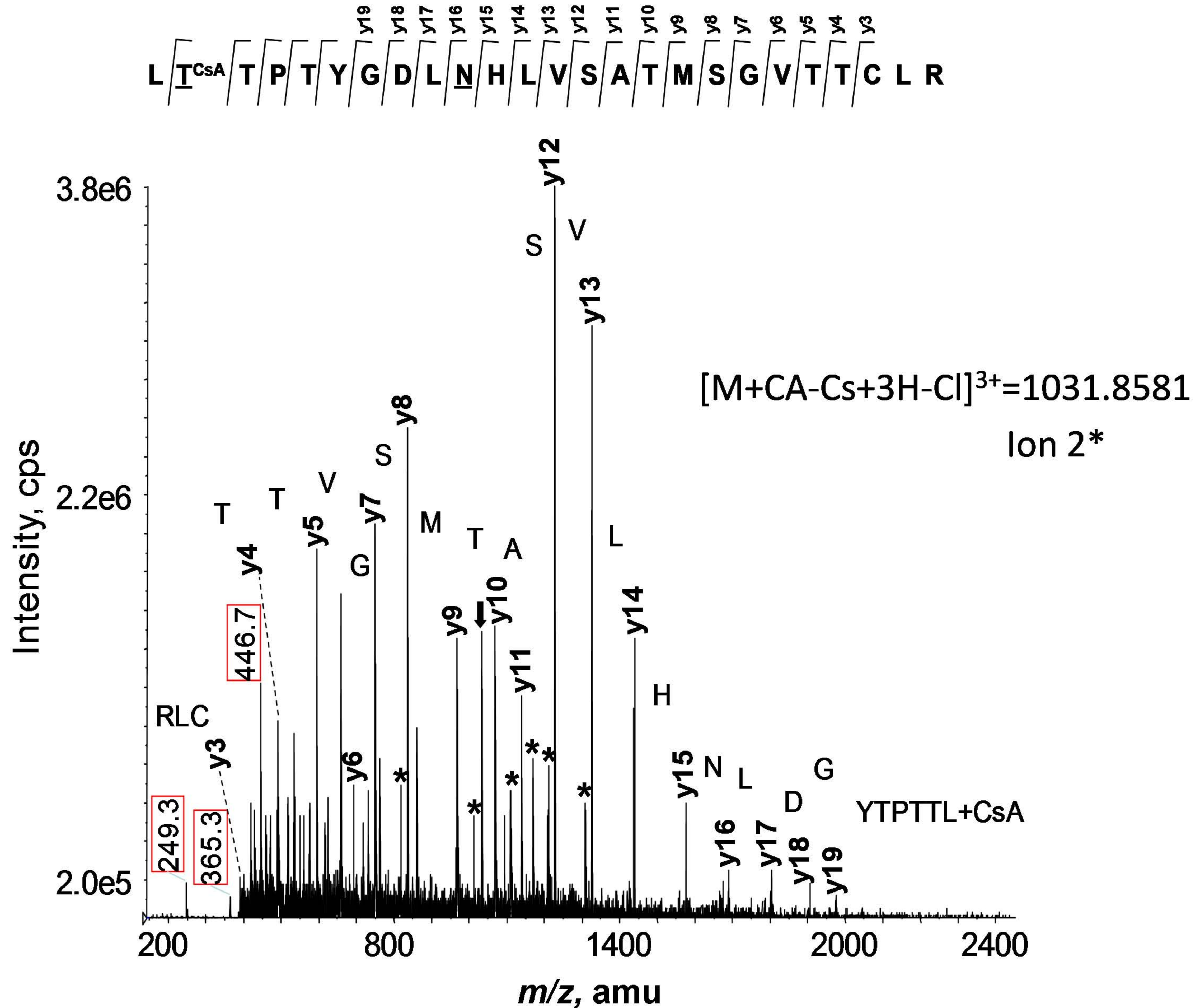


# Supplemental Figure 3



# Supplemental Figure 4





# Supplemental Figure 6

XIC 1017.855; 1031.186

